Supporting Information Appendix

Orally Administrable Therapeutic Synthetic Nanoparticle for Zika Virus

Bapurao Surnar,[a,b] Mohammad Z. Kamran,[a,b§] Anuj S. Shah,[a§] Uttara Basu,[a] Nagesh Kolishetti,[a,f] Sapna Deo,[a,c] Dushyantha T. Jayaweera,[d,e] Sylvia Daunert,[a,b,c,d] and Shanta Dhar[a,b,c]*

a. Department of Biochemistry and Molecular Biology, Leonard M. Miller School of Medicine, University of Miami, 1011 NW 15th St, Miami, FL 33136, USA

b. Dr. JT Macdonald Foundation Biomedical Nanotechnology Institute of the University of Miami, Leonard M. Miller School of Medicine, University of Miami, 1951 NW 7th Ave, Suite 475, Miami, FL 33136, USA

c. Sylvester Comprehensive Cancer Center, Leonard M. Miller School of Medicine, University of Miami, 1475 NW 12th Ave, Miami, FL 33136, USA

d. University of Miami Clinical and Translational Science Institute, Leonard M. Miller School of Medicine, University of Miami, 1120 NW 14th St, Suite 710, Miami, FL 33136, USA

e. Department of Medicine, Miami Center for AIDS Research, Leonard M. Miller School of Medicine, University of Miami, 1580 NW 10th Ave, Miami, FL 33136, USA

f. Department of Immunology and Nano-Medicine, Herbert Wertheim College of Medicine, Florida International University, Miami, FL, 33199, USA

[§]M.Z.K. and A.S.S. contributed equally to this work.

*To whom correspondence should be addressed.

E-mail: shantadhar@med.miami.edu

Materials: All chemicals were used as received without further purification unless otherwise mentioned. Ivermectin, N, N′-dicyclohexylcarbodiimide (DCC), 4-dimethylaminopyridine (DMAP), N-hydroxysuccinimide (NHS), 6-aminohexanoic acid, maleic anhydride, N,N-diisopropylethylamine (DIPEA), sucrose, and D-(+)-trehalose dihydrate were purchased from Sigma-Aldrich. Acid terminated poly(DL-lactide-co-glycolide) (PLGA-COOH) of inherent viscosity dL/g, 0.15 to 0.25 was purchased from Durect LACTEL® absorbable Polymers. Polyethylene glycol (H_2N-PEG_{2000}-NH_2) was procured from JenKem Technology USA. Deuterated solvents, $CDCl_3$ and DMSO-d6 were purchased from Cambridge Isotope Laboratories Inc. Regenerative cellulose membrane Amicon Ultra centrifugal 100 kDa filters were purchased from Merck Millipore Ltd. Strata C18-T columns (catalog number 8B-S004-EAK) were purchased from Phenomenex. Copper grids for transmission electron microscopy (TEM) were purchased from Electron Microscopy Sciences. Qdot® 705 ITK™ Amino (PEG) Quantum Dots (catalog number Q21561MP) and ProLong® Gold anti-fade reagent with 4',6-diamidino-2-phenylindole (DAPI) were purchased from Life Technologies. Trans-well system polycarbonate (0.4-μm pore size, 12-well plates) were purchased from Corning, Lowell, MA. The tight junction antibody ZO-1 (catalog number ab59720) was purchased from Abcam. Alexa Fluor 488 goat anti-rabbit IgG secondary antibody (catalog number A11008) was procured from Invitrogen, ThermoFisher Scientific. Phosphate buffered saline (1X PBS) was purchased from Gibco (reference number 10010-023). Goat serum was obtained from Sigma Aldrich (catalog number G9023). Glutamine, penicillin/streptomycin trypsin-EDTA solution, HEPES buffer (1 M in water), and sodium pyruvate were procured from Sigma Life Sciences. Dulbecco's Modified Eagle's medium

(DMEM) and fetal bovine serum (FBS) were purchased from Gibco Life Technologies. Mouse monoclonal IgG, Fc-Rn (A-6) (Catalog number SC-393064) was purchased from Santa Cruz Biotechnology. Zika virus NS1 antibody (EA88) (catalog number. MA5-24583) was purchased from Invitrogen. Flag-tagged Zika NS1 plasmid (Catalog number 79641) was procured from Addgene. Native human IgG FC fragment protein (catalog number Ab90285) was procured from Abcam. Ammonium persulfate (Catalog number 161-0180), tris/glycine/SDS buffer (Catalog number 161-0732), SDS-PAGE gel preparation kit TGX stain-free™ fast cast™ acrylamine 10% (Catalog number 161-0182), and Clarity™ western ECL substrate (Catalog number 170-5060) were purchased from Bio-Rad Inc. Beta-actin antibody (Catalog number ab8226), nitrocellulose membrane (catalog number 88018), and tween-20 was purchased from Fisher Bioreagents. Simulated gastric fluid (SGF) was purchased from Ricca chemical and Omeprazole was procured from Sigma.

Instruments: ^{1}H and ^{13}C NMR spectra were recorded on 400 MHz Bruker NMR spectrometer. Gel permeation chromatographic (GPC) analyses were performed on Shimadzu LC20-AD prominence S4 liquid chromatographer equipped with a refractive index detector and water columns; molecular weights were calculated using a conventional calibration curve constructed from narrow polystyrene standards using DMF as an eluent at a temperature of 40 °C. Dynamic light scattering (DLS) measurements were carried out using a Malvern Zetasizer Nano ZS system. Distilled water was purified by passage through a Millipore Milli-Q Biocel water purification system (18.2 MΩ) containing a 0.22 μm filter. Absorbance analyses were performed on a Bio-Tek Synergy HT microplate reader. High-performance liquid chromatography (HPLC) analyses were

made on an Agilent 1200 series instrument equipped with a multi-wavelength UV-visible and a fluorescence detector. Cells were counted using Countess® Automated Cell Counter procured from Invitrogen. TEM images were acquired using a JEOL JEM-1400 equipped with a Gatan Orius SC 200D CCD digital camera with a magnification of 80K. Inductively coupled plasma mass spectrometry (ICP-MS) studies were performed on an Agilent 7900 ICP-MS instrument. Mitochondrial bioenergetics assays were performed on XF^e96 Extracellular Flux Analyzer (Agilent Seahorse Biosciences). TEER measurements were performed on a Millicell® ERS-2 Voltohmmeter Instrument (Catalog number MERS00002) purchased from Millipore. Confocal microscopy images were obtained using an Olympus FluoView FV3000. H and E images were captured using a Zeiss Stemi 2000-CS stereoscope fitted with a CL-1500 ECO SteREO light source.

Table S1. Literature Reported Ivermectin-loaded Nanoformulations

	Title	Citation	Procedure used in synthesis of NPs	Type of NPs	Size (nm) Zeta potential (mV)	% Loading % EE	Application	Shortcomings
1	Polyanhydride Nanoparticle Delivery Platform Dramatically Enhances Killing of Filarial Worms	*PLoS Negl Trop Dis* **2015**, 9 (10); e0004173	Solid/oil/oil nanoprecipitation	Microparticles	250 Not provided	5% Not Provided	Reduce the microfilaria	• Incomplete characterizatio of NPs • Non-spherical NPs • Large size • No targeting ability • No antiviral activity
2	Lipid Nanostructured Carriers Systems for Ivermectin and Methoprene Aiming Parasite Control	*Quím. Nova.* **2016**, vol.39, n.9, pp.1034-1043	Nanoprecipitation	Lipid nanoparticles	210 Not provided	7% Not provided	Anti-parasitic treatment	• Incomplete characterization of NPs • Large size • No targeting ability • No antiviral activity
3	Ivermectin-loaded solid lipid nanoparticles: preparation, characterization, stability and transdermal behavior	*Artificial cells, Nanomedicine and Biotechnology*, **2018**, 46 (2), 255	Hot homogenization	Lipid nanoparticles	312 -30	10% 98%	Treatment of scabies.	• Incomplete characterization of NPs • Large size • No targeting ability • No antiviral activity
4	Ivermectin-Loaded Polymeric Nanoparticles: Screening the Effects of Polymers, Methods, and the Usefulness of Mathematical Models	Journal of Nanoscience and Nanotechnology, **2017**, 17(6), pp. 4218-4234	Nanoprecipitation	Nanocapsules	200 -30	3% Not provided	Used to study Korsmeyer-Peppas's generalized equation	• Incomplete characterization of NPs • Only mathematical models, no biological experimental evaluation
5	Ivermectin-loaded lipid nanocapsules: toward the development of a new antiparasitic delivery system for veterinary applications	*Parasitology Research* **2016**, 115(5), 1945-53	Hot homogenizations	Lipid nanocapsules	55 -17	Not provided 98%	Anti-parasitic treatment	• Incomplete characterization of NPs • No targeting ability • No antiviral activity
6	Liposomal Systems as Nanocarriers for the Antiviral Agent Ivermectin	International Journal of Biomaterials Volume 2016, Article ID 8043983	Ethanol injection	Liposomes	30 to 350 Not provided	Not provided 98%	To treat Dengue Virus	• No targeting ability • Limited translational use due to large size
7	Design and in vitro characterization of ivermectin nanocrystals	*Pharm Dev Technol. 2017 Sep;22(6):809-817*	Emulsification	Nano suspensions	215 Not provided	1% Not provided	NP synthetic model	• No targeting ability • Not biodegradable
8	Safety test of Ivermectin nanoemulsion on beef cattle	*Guangdong Nongye Kexue (2014), 41(2), 125-127*	Emulsification	Nano suspensions	Not provided	2% Not provided	Safety study	• Incomplete characterization of NPs • No targeting ability • No antiviral activity
9	Preparation and property evaluation of ivermectin nanoemulsion for injection	*Xumu Shouyi Xuebao (2011), 42(8), 1161-1167*	Emulsification	Nano suspensions	Not provided	5% Not provided	NP synthetic model	• No targeting ability • Not biodegradable • No pharmaceutical application
10	Ivermectin lipid-based nanocarriers as novel formulations against head lice	*Parasitology research (2017), 116(8), 2111-2117*	Phase inversion procedure	Nanocapsules	55 Not provided	0.11% Not provided	Against head lice	• Incomplete characterization of NPs • No targeting ability • No antiviral activity
11	Therapeutic efficacy of poly (lactic-co-glycolic acid) nanoparticles encapsulated ivermectin (nanoivermectin) against Brugian filariasis in experimental rodent model	*Parasitology research (2014), 113(2), 681-91*	Nanoprecipitation	Nano-IVM	96 Not provided	74% Not provided	Brugian filariasis	• Incomplete characterization of NPs • No targeting ability • No antiviral activity

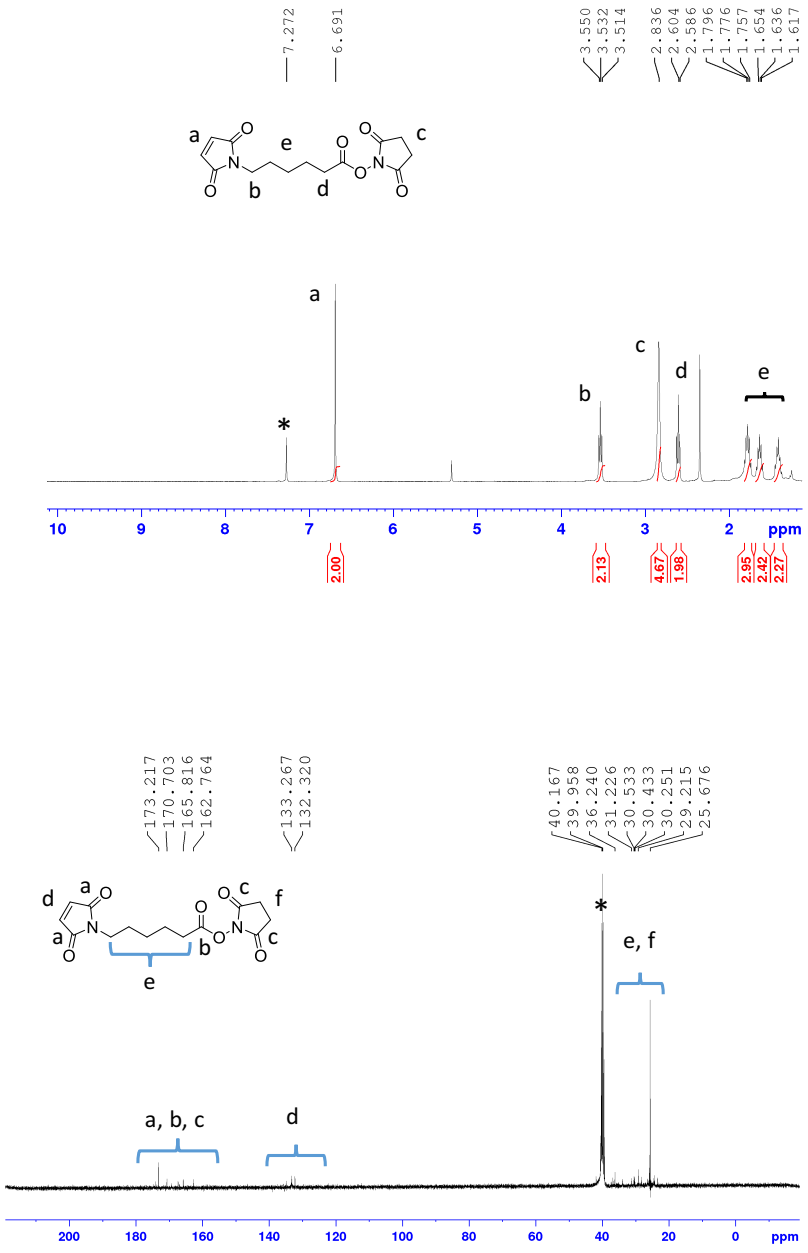

Figure S1. (A) ^{1}H NMR and (B) ^{13}C NMR of MAL-NHS in $CDCl_3$.

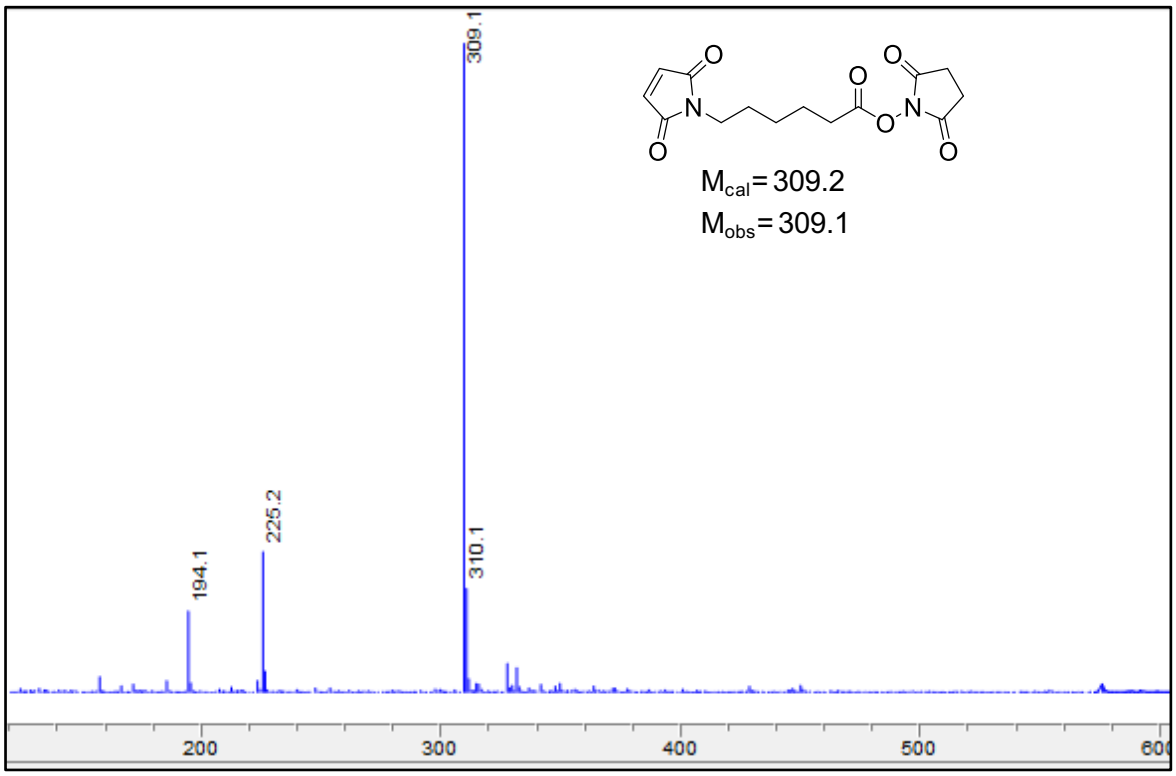

Figure S2. LC-MS-ESI of MAL-NHS.

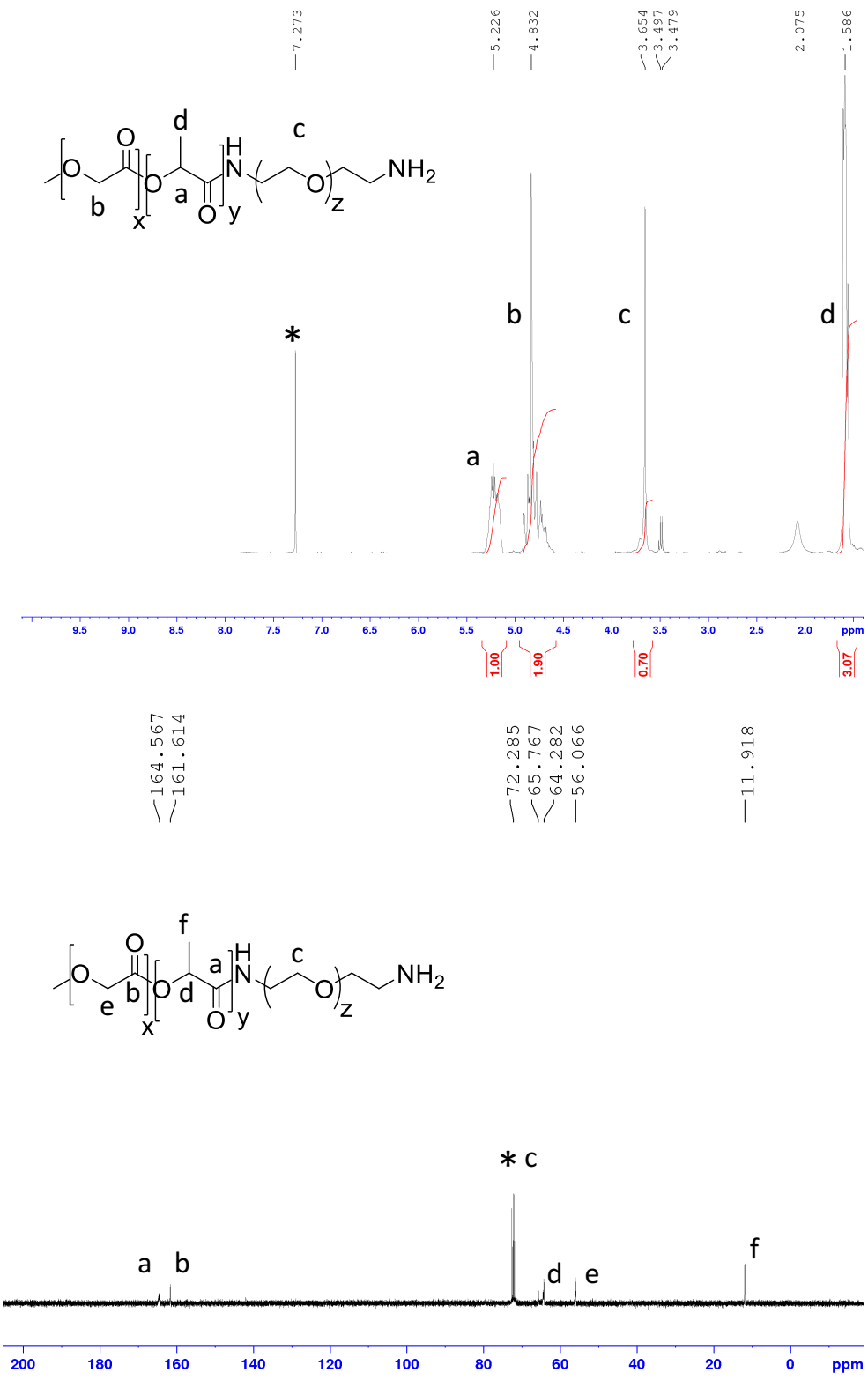

Figure S3. (A) ^{1}H NMR and (B) ^{13}C NMR of PLGA-*b*-PEG-NH_2 in $CDCl_3$.

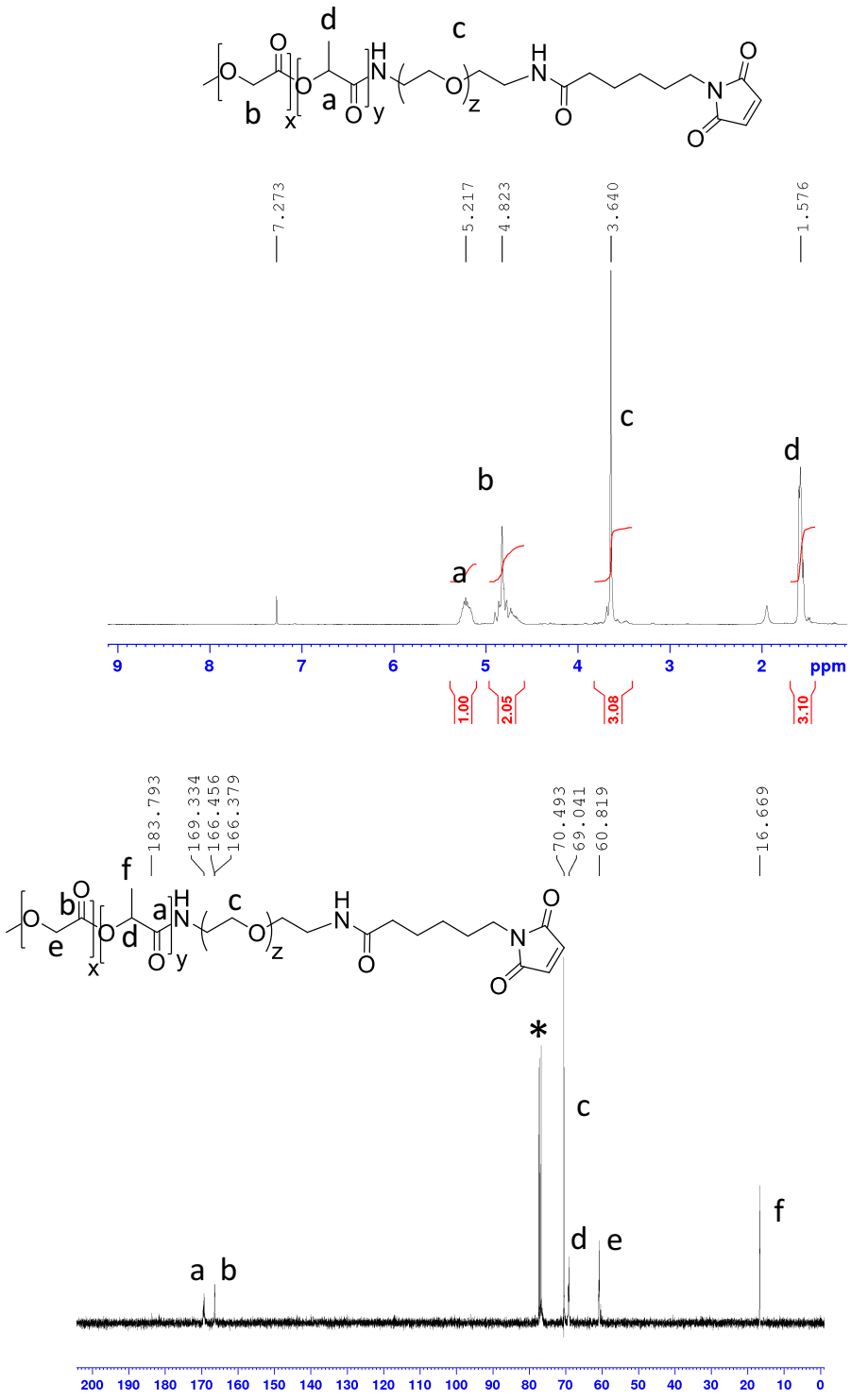

Figure S4. (A) ^{1}H NMR and (B) ^{13}C NMR of PLGA-*b*-PEG-MAL in $CDCl_3$.

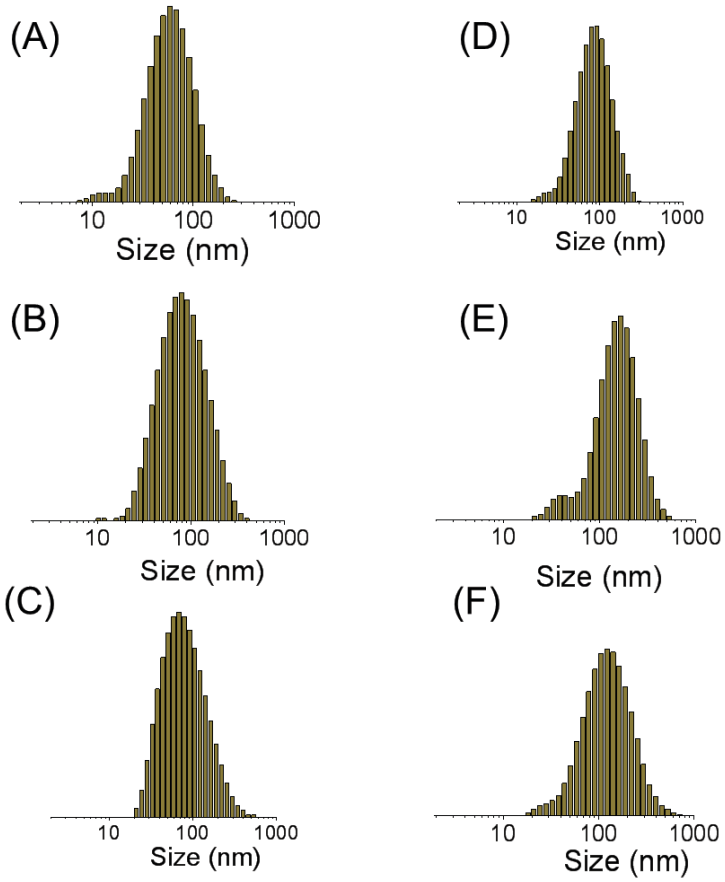

Figure S5. DLS histograms of (A) Mal-NP, (B) Mal-IVM10-NP, (C) Mal-IVM20-NP, (D) Mal-IVM30-NP, (E) Mal-IVM40-NP and (F) Mal-IVM50-NP in nanopure water at 37° C.

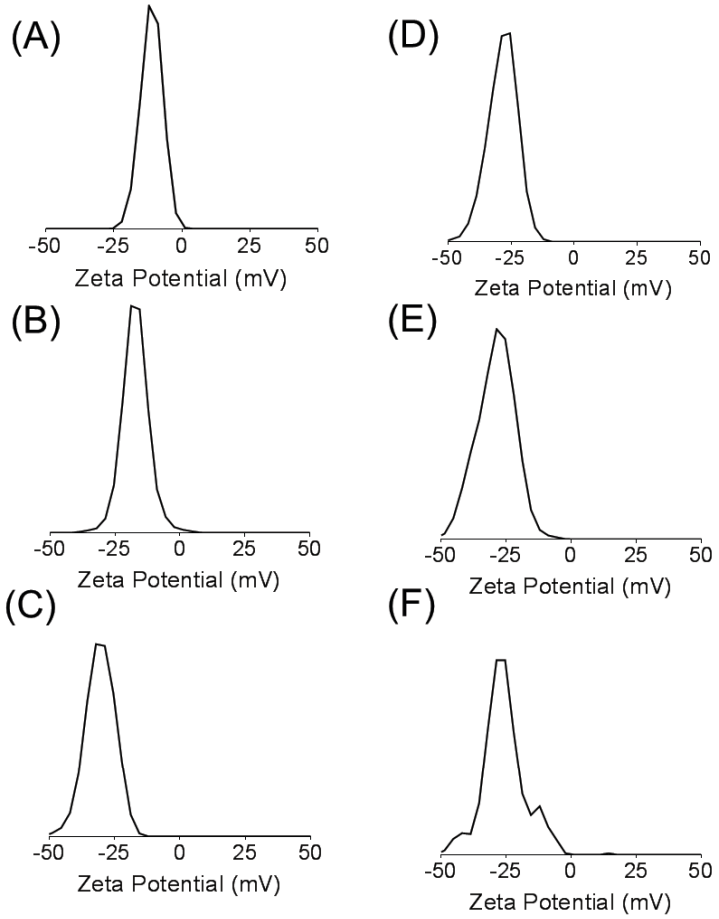

Figure S6. Zeta potential (mV) of (A) Mal-NP, (B) Mal-IVM10-NP, (C) Mal-IVM20-NP, (D) Mal-IVM30-NP, (E) Mal-IVM40-NP and (F) Mal-IVM50-NP in nanopure water at 37° C.

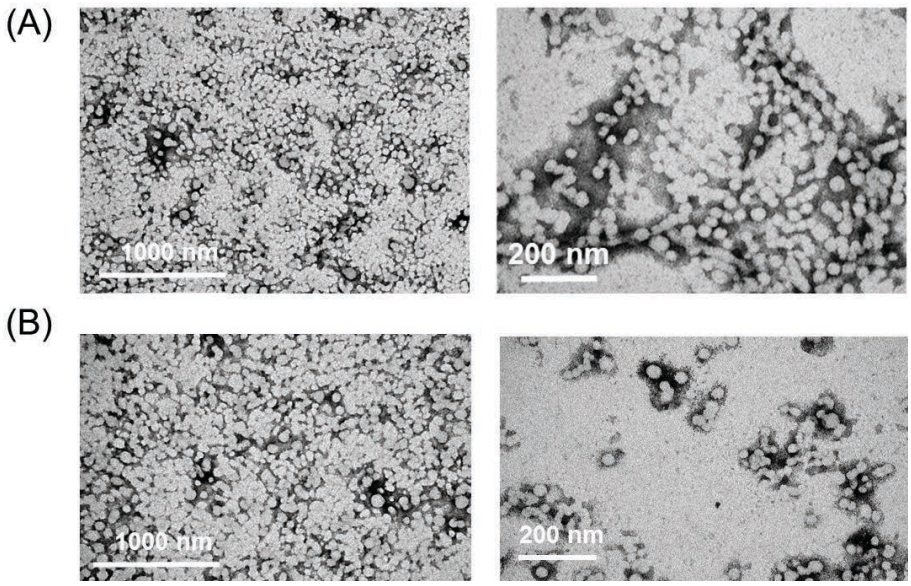

Figure S7. TEM images of (A) NT-Mal-NP and (B) NT-Mal-IVM-NP stained with 4% of uranyl acetate.

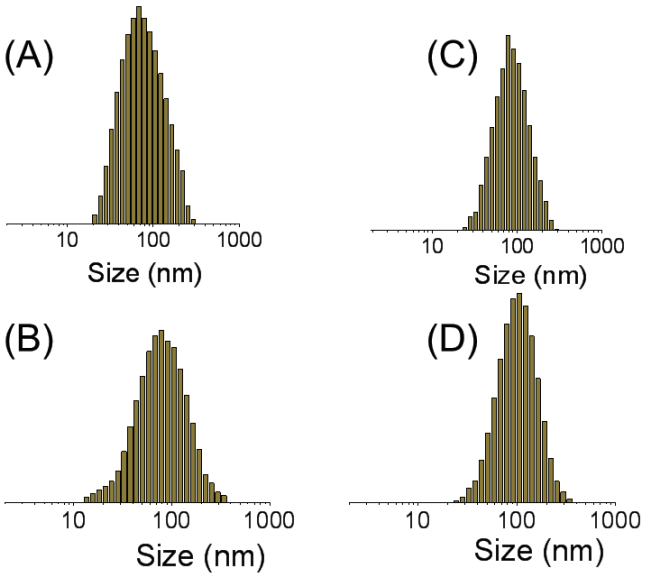

Figure S8. (A) DLS histograms of (A) NT-Mal-NP, (B) T-Fc-NP, (C) NT-Mal-IVM-NP, and (D) T-Fc-IVM-NP in nanopure water at 37° C.

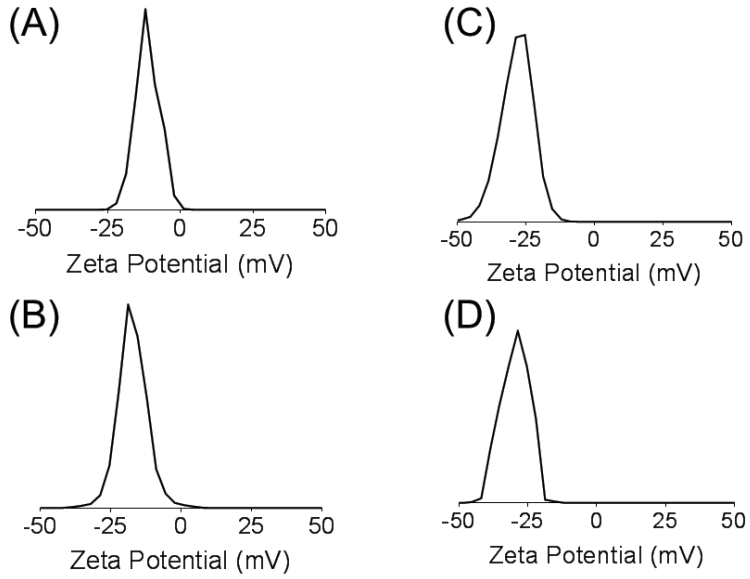

Figure S9. Zeta potential (mV) of (A) NT-Mal-NP, (B) T-Fc-NP, (C) NT-Mal-IVM-NP, and (D) T-Fc-IVM-NP in nanopure water at 37° C.

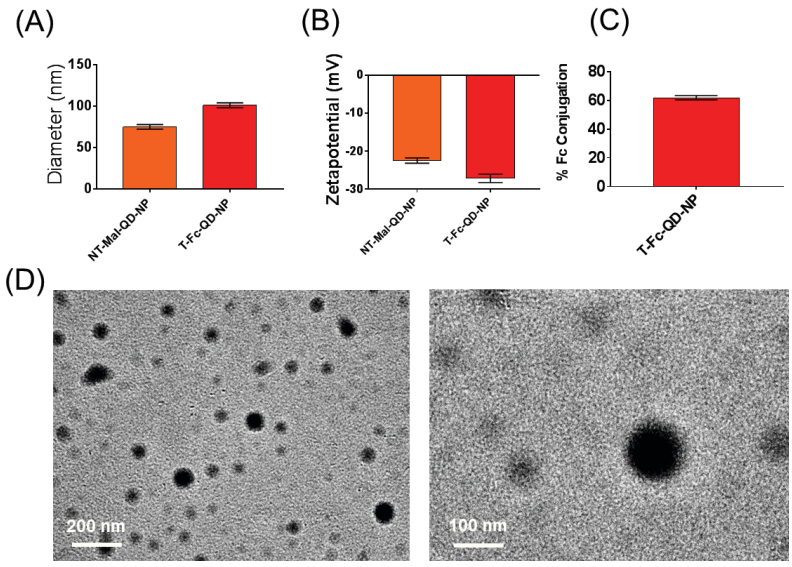

Figure S10. (A) Diameters, (B) Zeta potentials of NT-Mal-QD-NP and T-Fc-QD-NP. (C) Fc conjugation efficiency of targeted NPs by the bicinchoninic acid assay (BCA). (D) TEM images of T-Fc-QD-NP (unstained)

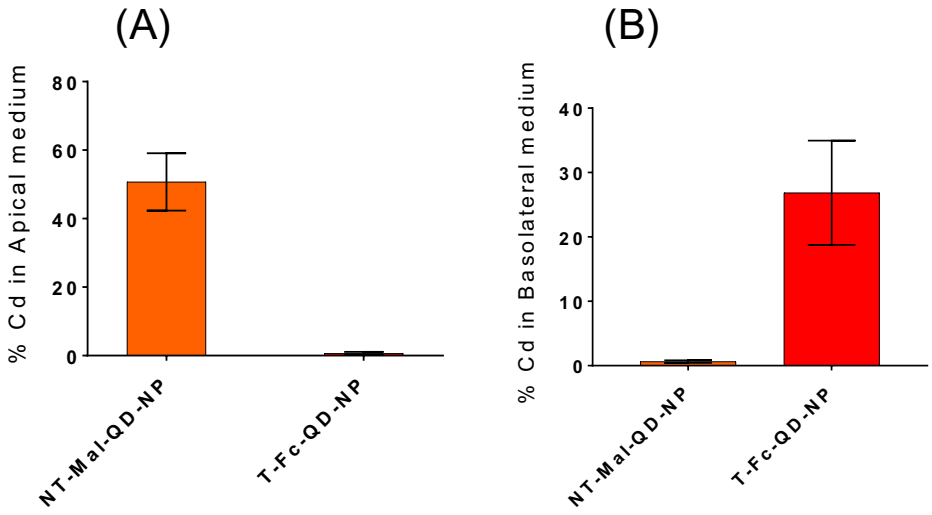

Figure S11. Quantification of QD (Cd) loaded NPs in the (A) apical and (B) basolateral sides of the endothelial cell barrier.

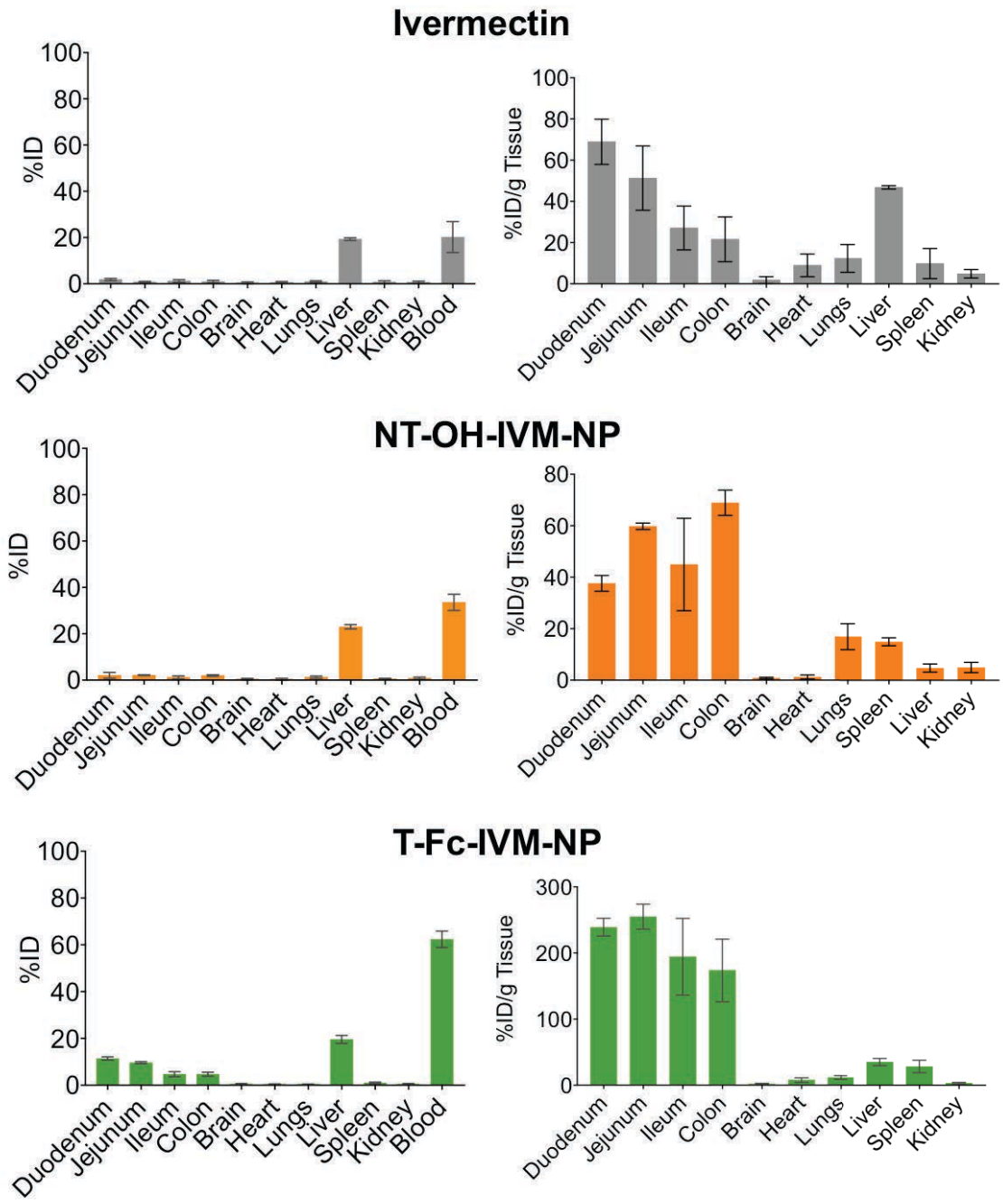

Figure S12. Biodistribution of ivermectin, NT-OH-IVM-NP, T-Fc-IVM-NP after oral administration to Balb/c albino mice. Data are mean %ID per gram of tissue ± SD (n = 3 mice per group).

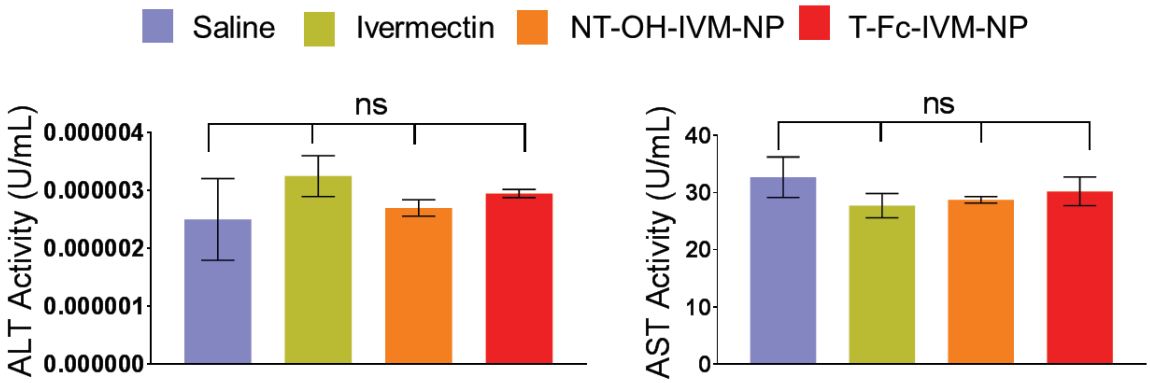

Figure S13. Alanine aminotransferase (ALT) and Aspartate Aminotransferase (AST) levels from the blood plasma of BALB/c mice (n=3 in each group) treated with single dose of articles (at a dose of 40 mg/kg with respect to ivermectin) *via* oral gavage for 24 h.

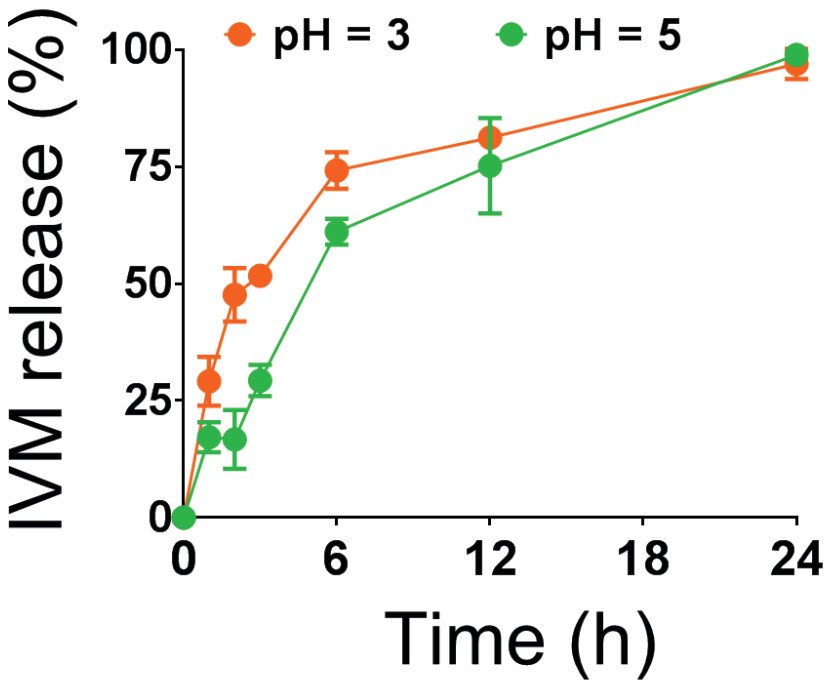

Figure S14. Release of IVM from NT-Mal-IVM-NPs at pH 3 and 5 at 37 °C

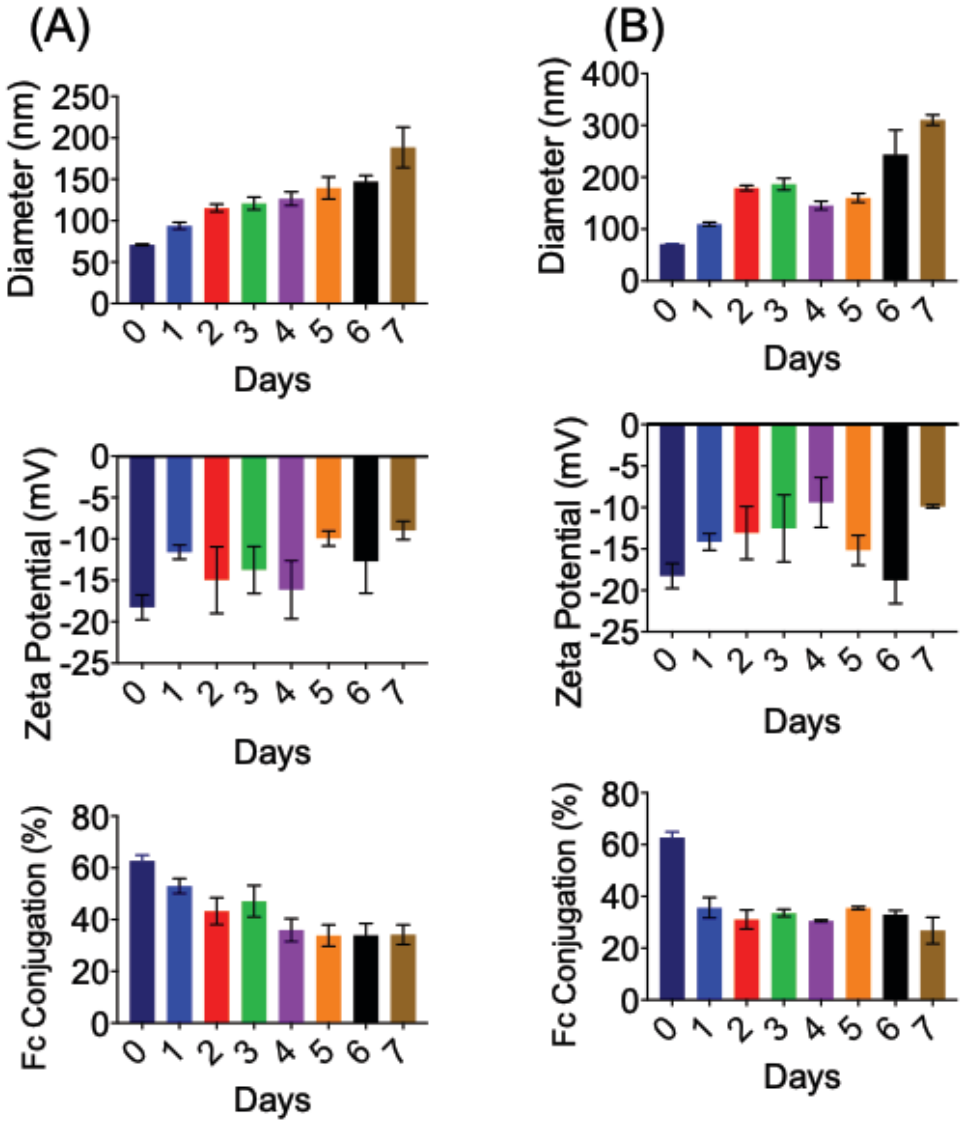

Figure S15. Stability of T-Fc-IVM-NP in simulated gastric fluid (SGF) at (A) room temperature and (B) 37 °C.

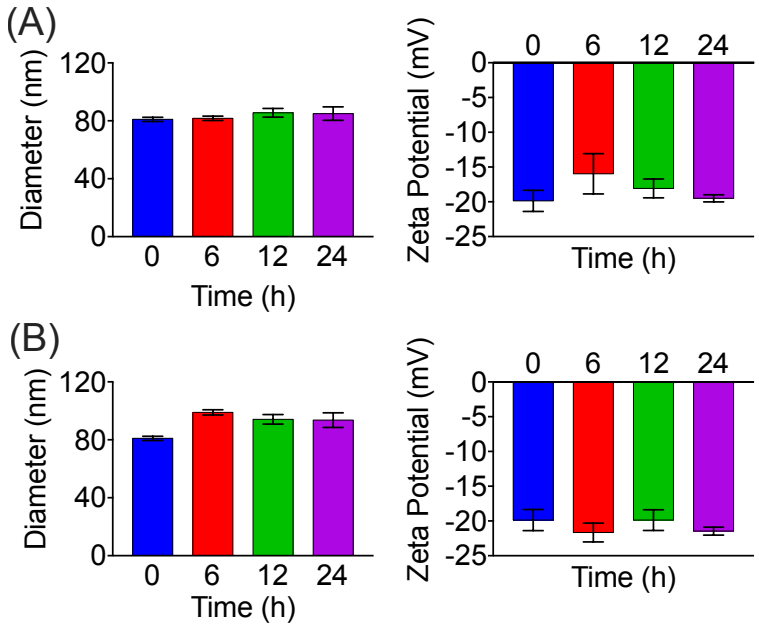

Figure S16. Stability of NT-Mal-IVM-NP in simulated gastric fluid (SGF) without (A) and with (B) Omeprazole at room temperature.

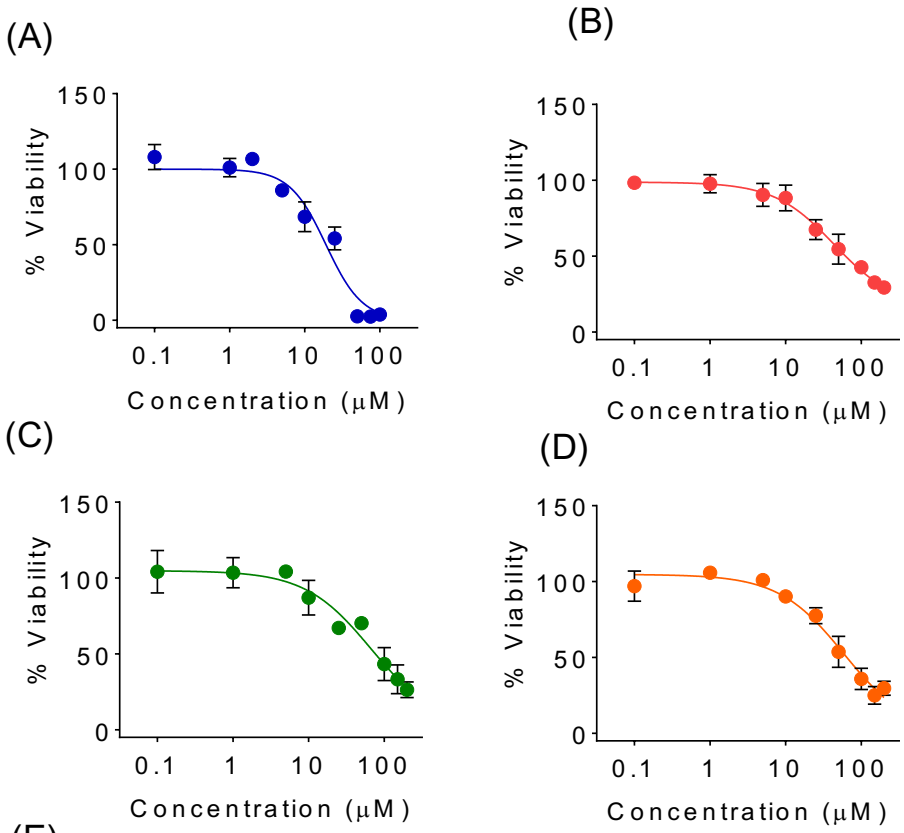

(E)

Articles	IC_{50} Value (μM)
Ivermectin	19.1 ± 4.2
NT-OH-IVM-NP	66.5 ± 7.1
NT-MAL-IVM-NP	43.2 ± 6.0
T-Fc-IVM-NP	60 ± 3.2

Figure S17. *In vitro* efficacy of (A) ivermectin, (B) NT-OH-IVM-NP, (C) NT-Mal-IVM-NP, and (D) T-Fc-IVM-NP in Caco-2 cells by the MTT assay. (E) IC_{50} values of the articles in the Caco-2 cells after treatment for 72 h.

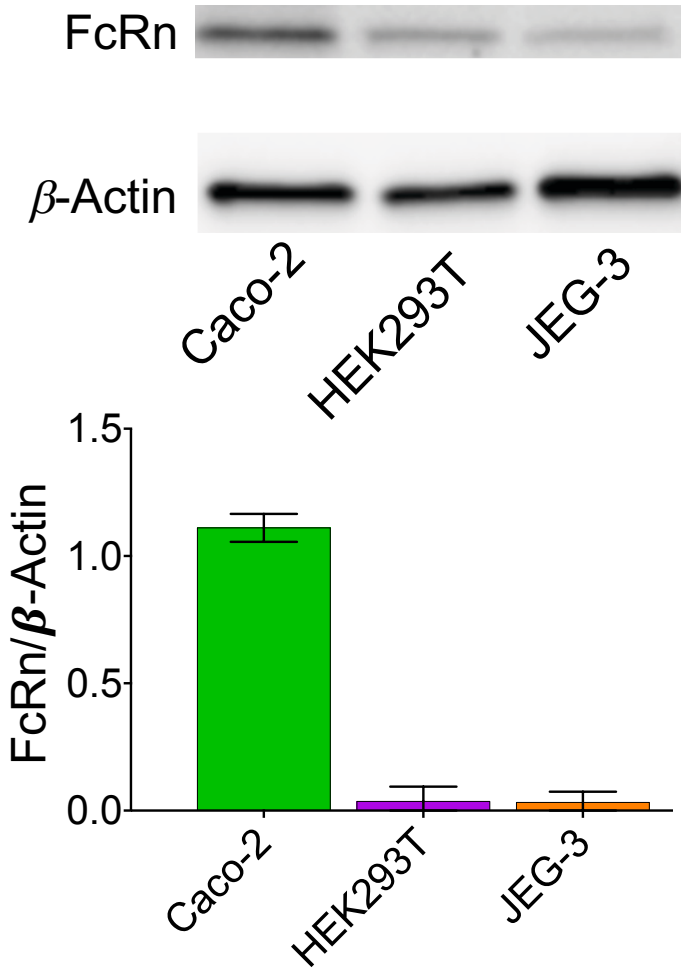

Figure S18. Comparison of FcRn expression level in Caco-2, HEK293T, and JEG-3 cells by western blotting.

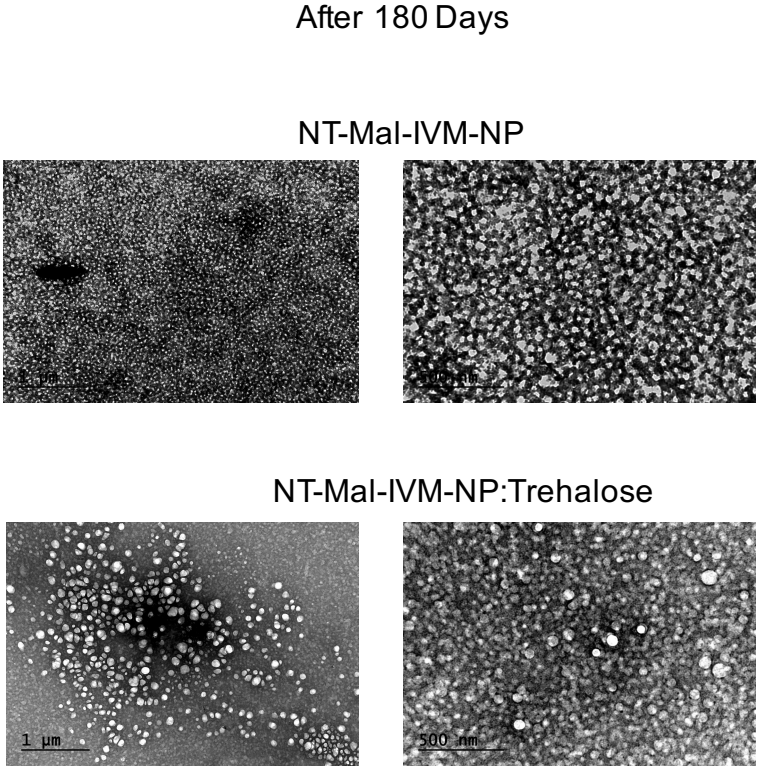

Figure S19. Morphological comparison of NT-Mal-IVM-NP and NT-Mal-IVM-NP with sucrose after 180 days by TEM.